

## Supporting Information

### Production of Functionalised Chitins Assisted by Fungal Lytic Polysaccharide Monooxygenase

Damao Wang<sup>a,b</sup>, Jing Li<sup>a</sup>, Germán Salazar-Alvarez<sup>b,c</sup>, Lauren S. McKee<sup>a,b</sup>, Vaibhav Srivastava<sup>a</sup>,  
Jonas A. Sellberg<sup>d</sup>, Vincent Bulone<sup>a,b,e,f</sup>, Yves S. Y. Hsieh<sup>a,b\*</sup>

<sup>a</sup> Division of Glycoscience, Department of Chemistry, School of Engineering Sciences in Chemistry, Biotechnology, and Health, KTH Royal Institute of Technology, AlbaNova University Center, Stockholm, SE106 91, Sweden.

<sup>b</sup> Wallenberg Wood Science Center, KTH Royal Institute of Technology, 100 44, Stockholm, Sweden

<sup>c</sup> Department of Materials and Environmental Chemistry, Arrhenius Laboratory, Stockholm University, SE-106 91 Stockholm, Sweden

<sup>d</sup> Biomedical and X-Ray Physics, Department of Applied Physics, AlbaNova University Center, KTH Royal Institute of Technology, SE-106 91 Stockholm, Sweden

<sup>e</sup> ARC Centre of Excellence in Plant Cell Walls, School of Agriculture Food and Wine, University of Adelaide, Waite Campus, Urrbrae, SA 5064, Australia

<sup>f</sup> Adelaide Glycomics, School of Agriculture Food and Wine, University of Adelaide, Waite Campus, Urrbrae, SA 5064, Australia

\* Corresponding author: Yves S. Y. Hsieh; Email: yvhsieh@kth.se

**Table S1** Primers used for cloning of *FfAA11*

Primer	Sequence (5'-3')
pelB leader Forward	CATATGAAATACCTGCTGCC
pelB- <i>FfAA11</i> Reverse	TCAGCATGTGGGCCATCGCC
pelB- <i>FfAA11</i> Forward	GGCGATGGCCCACATGCTGA
<i>FfAA11</i> Reverse	CTCGAGCGGTGCACCCCATG

**Table S2** XPS analyses

a) Relative surface composition in atomic %. The analysis depth is about 10 nm.

Sample	Atomic%									Atomic ratio
	C	O	N	S	F	Si	P	Na	Al	O / C
Chitin <i>ref.</i>	58.5	34.1	6.9	0.4	-	(0.1)	-	-	-	0.58
LPMO-treated chitin	58.6	33.5	7.2	-	0.6	0.2	-	-	-	0.57

- denotes that no signal was detected above the background noise level (about 0.05-0.1 atomic %)

( ) denotes a small peak, with signal close to the background noise level

b) Chemical shifts in the high-resolution carbon spectra, with the binding energy positions for each carbon peak after adjusting C1-carbon to 285.0 eV as the reference value. The chemical shifts are due to carbons in different functional groups with oxygen mainly (but some may be from functional groups between C and N). Values are from curve fitting of the different carbon peaks with the total amount of carbon set to 100 %.

Sample	C 1s tot = 100 %			
	C 1 285.0 eV	C 2 286.5 eV	C 3 288.0-1 eV	C 4 289.1-2 eV
Chitin <i>ref.</i>	15.0	56.0	25.4	3.6
LPMO-treated chitin	16.1	55.8	24.5	3.6

**Examples of functional groups:**

C1 (unoxidised): C-C, C=C, C-H

C2 (one bond to O): C-O, C-O-C

C3 (two bonds to O/N): O-C-O, C=O, N-C-O, N-C=O

C4 (three bonds to O/N): C(=O)OH, O-C=O, N-C(=O)-N

c) The table shows the total amount of carbon (in atomic %) found in the different carbon peaks (i.e. different functional groups, described above). Values were calculated from the XPS data in Tables S3 a) and b).

Sample	Atomic%				
	C <sub>tot</sub>	C 1	C 2	C 3	C 4
Chitin <i>ref.</i>	58.5	8.8	32.7	14.8	2.1
LPMO-treated chitin	58.6	9.4	32.7	14.4	2.1

**Table S3** XRD analysis based on Gaussian peak fits between 7.8° and 10.5° scattering angle ( $2\theta$ ), corresponding to the (020) crystal plane of  $\alpha$ -chitin. The crystallinity index (C.I.) was calculated according to  $C.I. = 1 - I_{am}/I_{(020)}$ , where  $I_{(020)}$  is the maximum intensity of the (020) peak obtained from the Gaussian peak fit and  $I_{am}$  is the amorphous baseline intensity at  $2\theta = 16^\circ$ .  $C.I. = -0.7529$  DD + 1.0397 with  $R^2 = 0.9924$ . The approximate size  $L$  of the crystal grains was estimated using the Scherrer equation:  $L = K\lambda / (\Delta_{(020)} \cos(\theta))$ , where  $K$  is a dimensionless shape factor assumed to be  $K = 0.9$  (*i.e.* spherical grains),  $\lambda = 1.5418 \text{ \AA}$  is the x-ray wavelength, and  $\Delta_{(020)}$  is the full width at half maximum (FWHM) of the (020) peak measured in radians. Instrument broadening is assumed to be negligible. The error bars correspond to a 95% confidence interval obtained from the Gaussian peak fit and propagated according to linear error propagation.

<b>Sample</b>	<b><math>I_{am}</math> (arb. u.)</b>	<b><math>I_{(020)}</math> (arb. u.)</b>	<b><math>\Delta_{(020)}</math> (rad)</b>	<b>C.I.</b>	<b>L (nm)</b>
<b>Chitin <i>ref.</i></b>	266	$1275 \pm 63$	$0.01381 \pm 7e-4$	$0.79 \pm 0.09$	$10.1 \pm 0.55$
<b>LPMO-treated chitin</b>	155	$719 \pm 47$	$0.01281 \pm 9e-4$	$0.78 \pm 0.18$	$10.9 \pm 0.81$

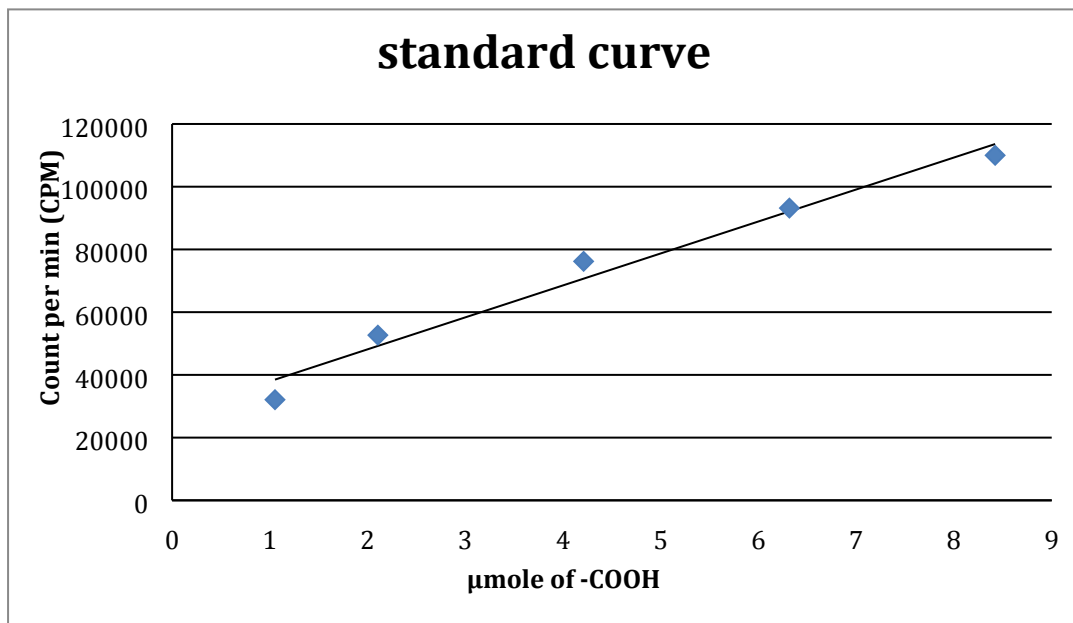
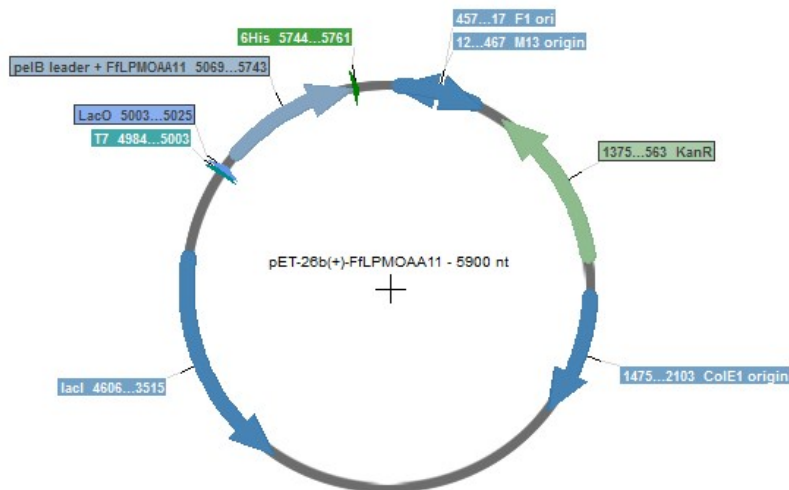


**Fig. S1** Standard curve of carboxyl groups produced using CM-cellulose, 50% substitution.



Vector map of pET-26b(+) harbouring *FfAA11* gene

Codon optimized sequence of amplified *FfAA11*

CATATGAAATACCTGCTGCCGACCGCTGCTGCTGGTCTGCTGCTCCTCGCTGCCAGCCGGCGATGGCC  
CACATGCTGATGGCAAATCCGAAACCGTATGGTAATCCGAATAACTTTCCGCTGGCAGCAGATGGTAG  
CGATTTTCCGTGTAAAGGTAAAGTTAATGATGGCAGCGGTGACAACGTGTATAAACAGGGTAGCACCC  
AGCAGCTGAGCTTTACCGGTCAGGCAGTTCATGGTGGTGGTAGCTGTCAGATTAGCCTGACCACCGAT  
AAAAATCCGACCAAAGATAGCGTTTGGAAAGTGATCAAAAGCATTGAAGGTGGTTGTCCGGCAAAG  
GTCAAGAGGGTAATATGGGTGATAATGCAGATGCACCGGATCCGTATAAATACGATTTTACCATTCCG  
AAAGAACTGGCAGCCGGTGAATATACCCTGGCATGGACCTGGTTTAAACAAAATTGGTAATCGCGAGAT  
GTACATGAATTGTGCAGCAGTTACCATTGAAGGCTCAGGTGGTAGCAAAGATCATCTGAATACCCTGC  
CGGATATGTTTGTGCAAATGTTGGTAATCAGTGTGAAACCCCGAGCGCAAAGATCTGGTTTTTCCGA  
ATCCGGTAATGATGTGGATAAATTCAATGGTGAACCGAAGCATGGGGTGCACCGCTCGAG

**Fig. S2** Vector map and sequence information

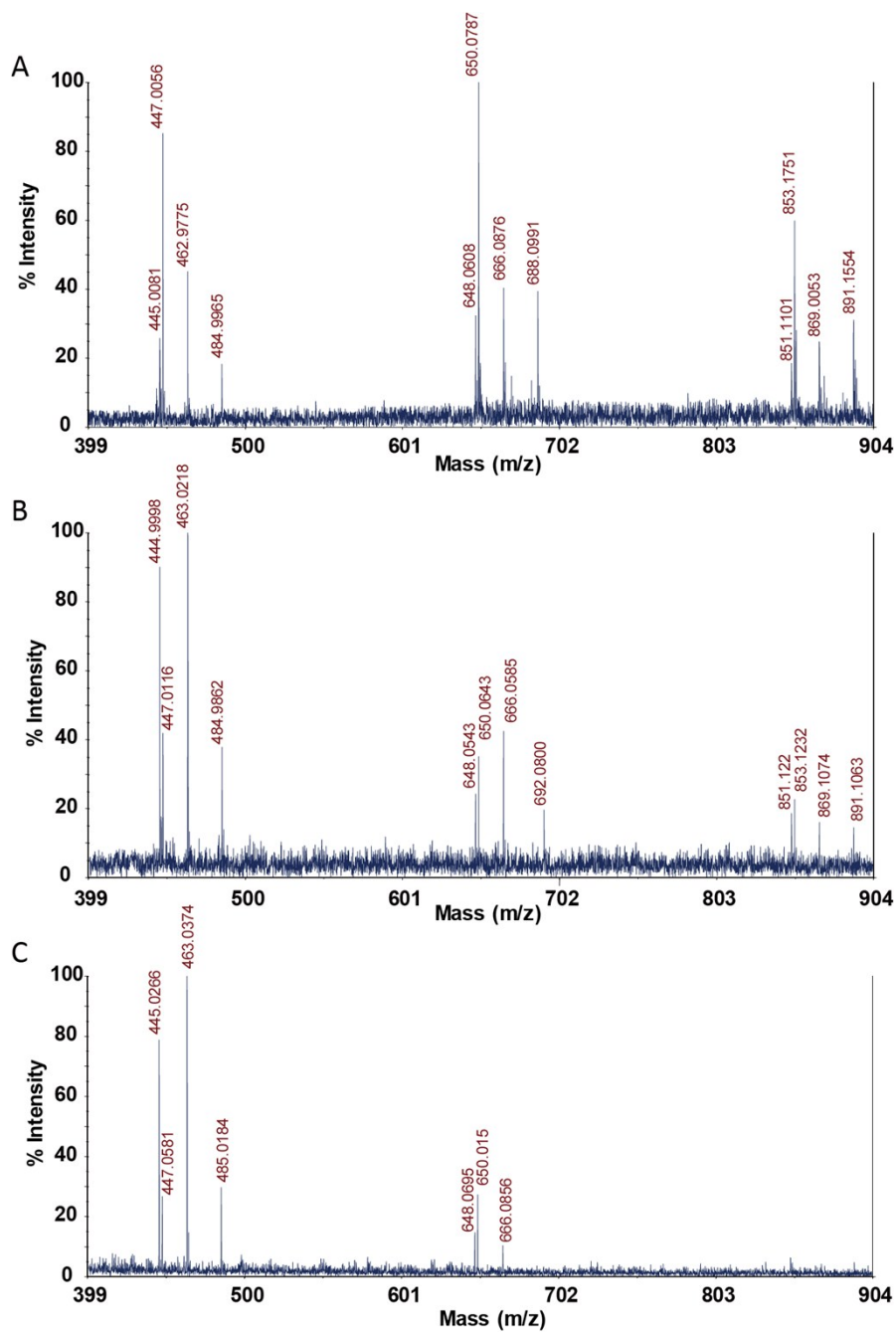


**Fig. S3** MALDI-TOF MS spectra of aldonic acid oligosaccharides derived from A)  $\alpha$ -chitin, B)  $\beta$ -chitin and C) lobster shell. (DP2/DP2<sub>-2</sub>/DP2<sub>+16</sub>, 445/447/463; DP3/DP3<sub>-2</sub>/DP3<sub>+16</sub>, 648/650/666; DP4/DP4<sub>-2</sub>/DP4<sub>+16</sub>, 851/853/869)

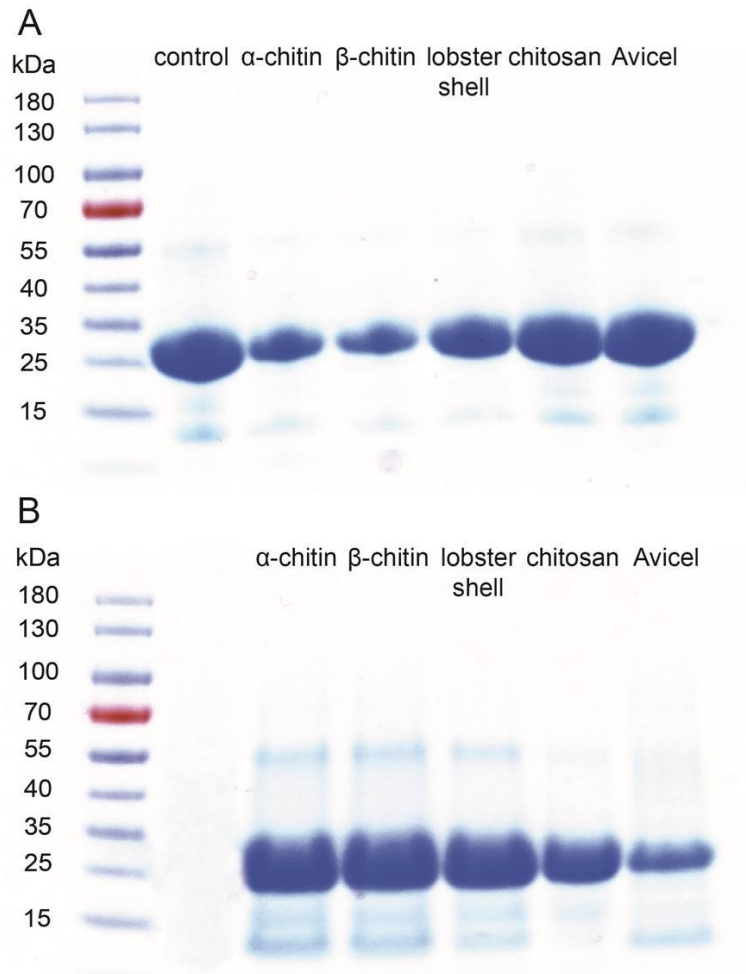


**Fig. S4** Binding assay of *FfAA11*, A) unbound protein in supernatant; B) protein bound to different substrates



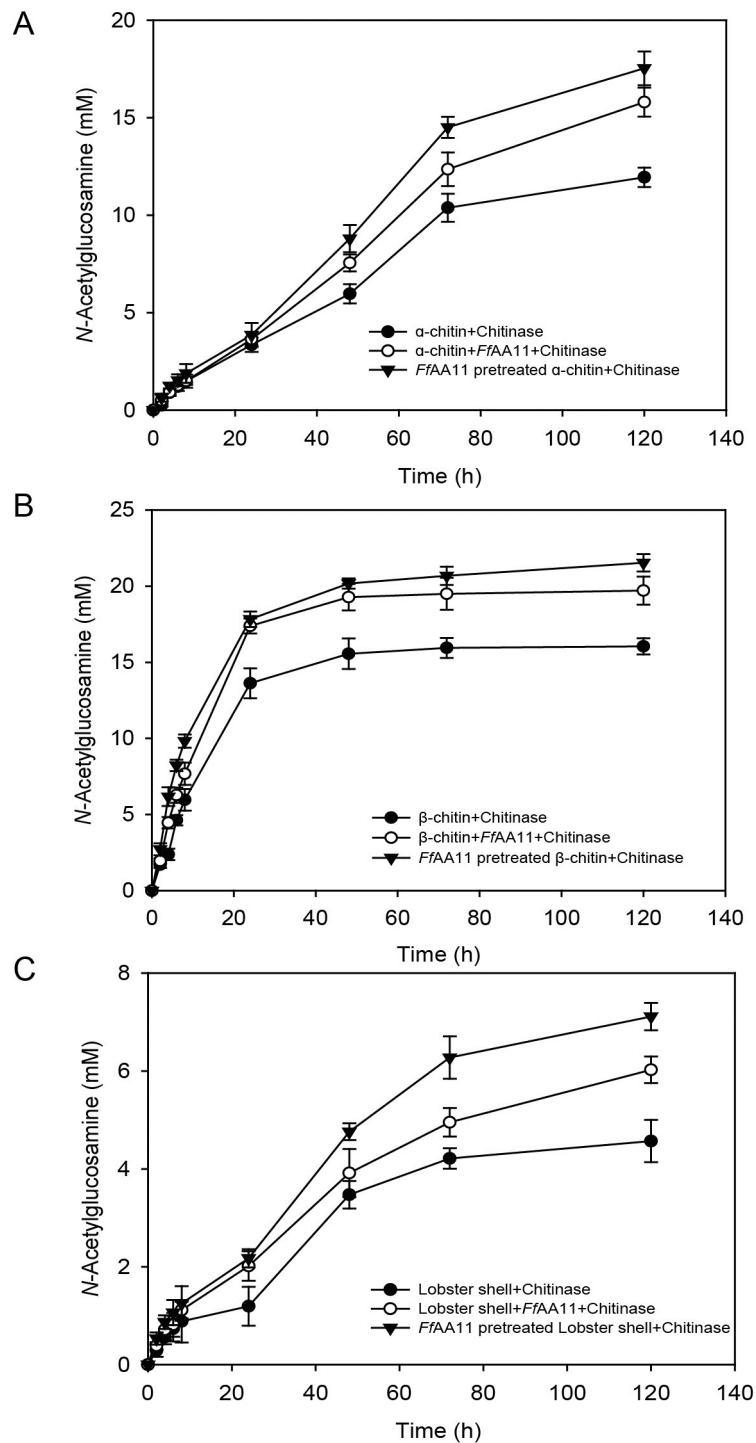


**Figure S5** GlcNAc production from  $\alpha$ - (A) and  $\beta$ -chitins (B), as well as lobster shells (C) after addition of *T. viride* chitinase and/or *FfAA11* for 2 h, 4 h, 8 h, 24 h, 72 h, 48 h, and 120 h reaction times.

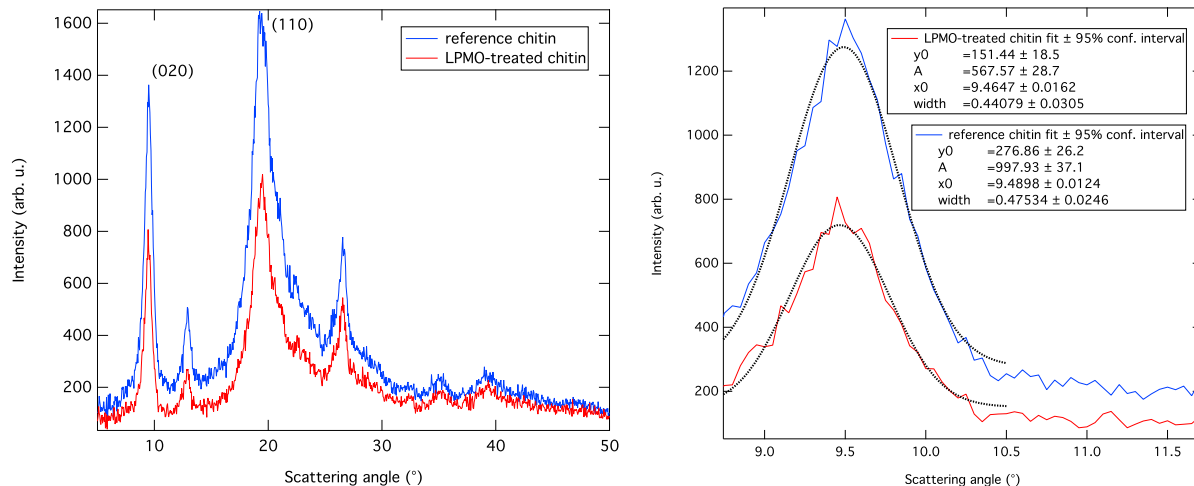


**Fig. S6** XRD measurements (left) of reference chitin (blue line) and LPMO-treated chitin (red line). The diffractograms are background normalised and the crystal planes of  $\alpha$ -chitin are labelled according to their Miller index for the two strongest peaks that are both perpendicular to the fiber axis. Gaussian peak fit (right) of the (020) peak (dotted black lines). The parameter values are given with a confidence interval of 95%. To relate to the parameters in Table S4,  $I_{(020)} = A + y_0$  and  $\Delta_{(020)} = \text{width} \cdot 2\sqrt{\ln(2)}$ .

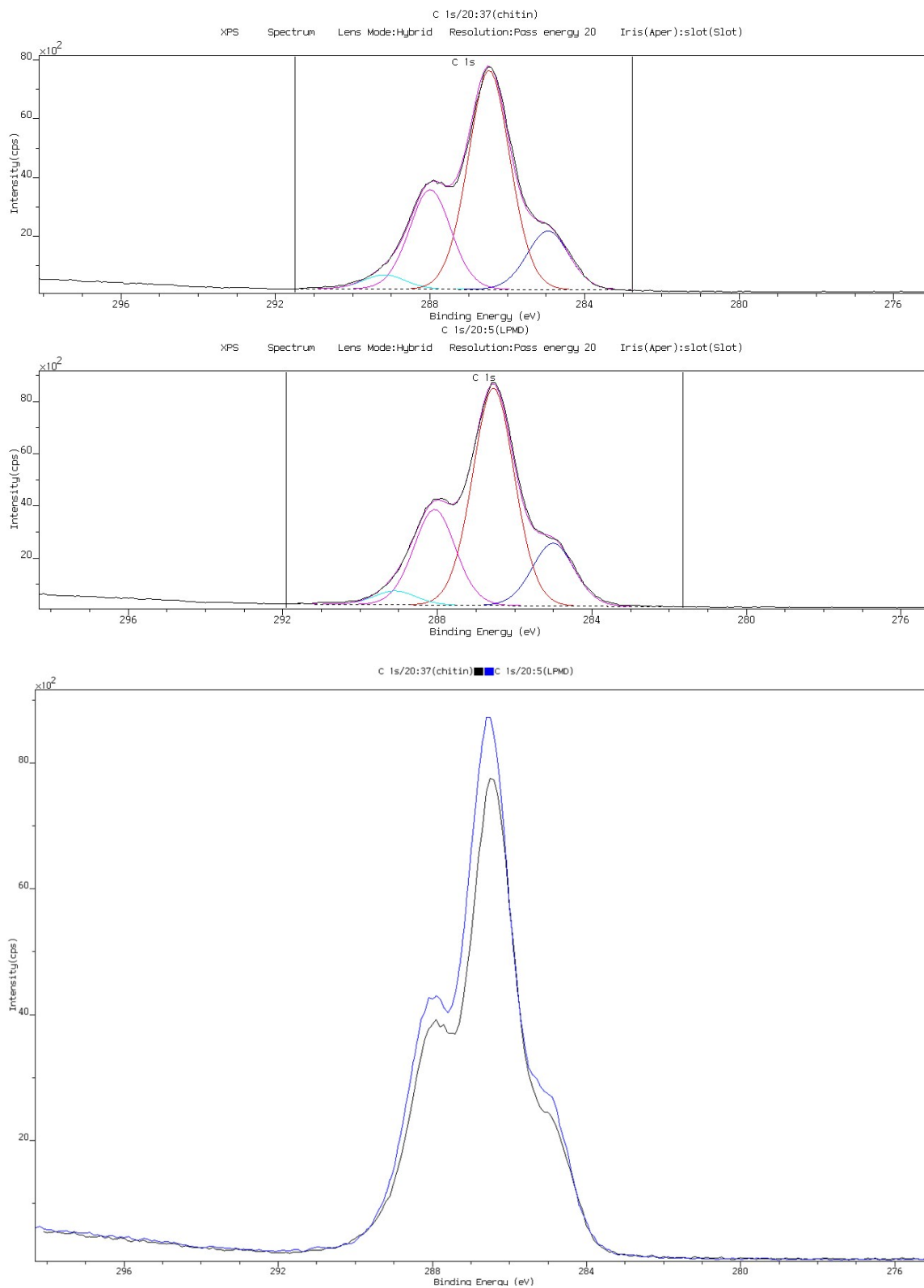


**Fig. S7** Curve-fitted high-resolved C 1s spectra of reference chitin (top) and LPMO-treated chitin (middle). The chemical shift relative to the reference binding energy of 285.0 eV depends on the oxidation state of the carbon atoms on the chitin surface (higher oxidation state results in higher

binding energy, see Table S3). The C4-carbon peak at 289.1 eV (cyan line) represents carboxyl groups (among other functional groups with 3 bonds to O/N) and corresponds to only 3.6% of all carbon on the chitin surface for both the reference and LPMO-treated chitin. XPS comparison (bottom) between C 1s spectra of reference chitin (black) and LPMO-treated chitin (blue).

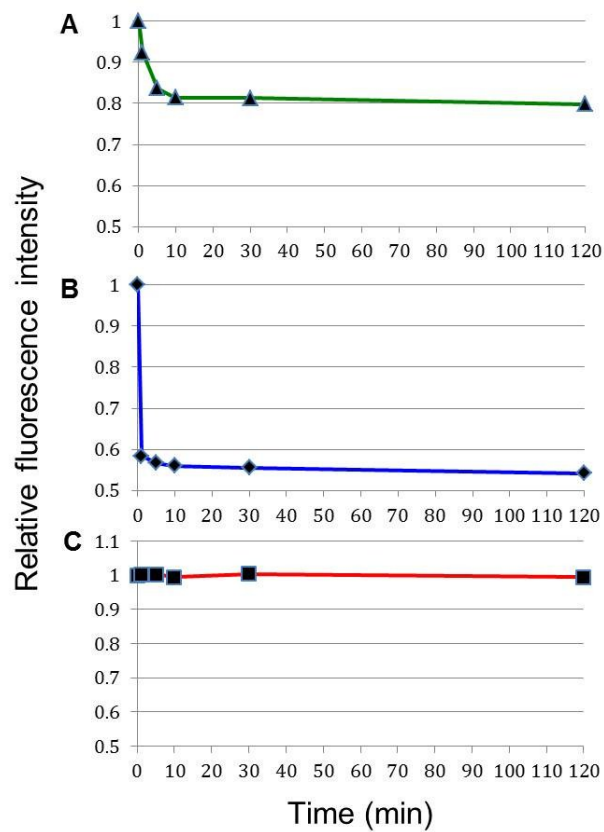


**Fig. S8** Fluorescent (FTSC) depletion of different coupling methods. A) COMU as coupling reagent. B) PyBOP as coupling reagent. C) FTSC only.

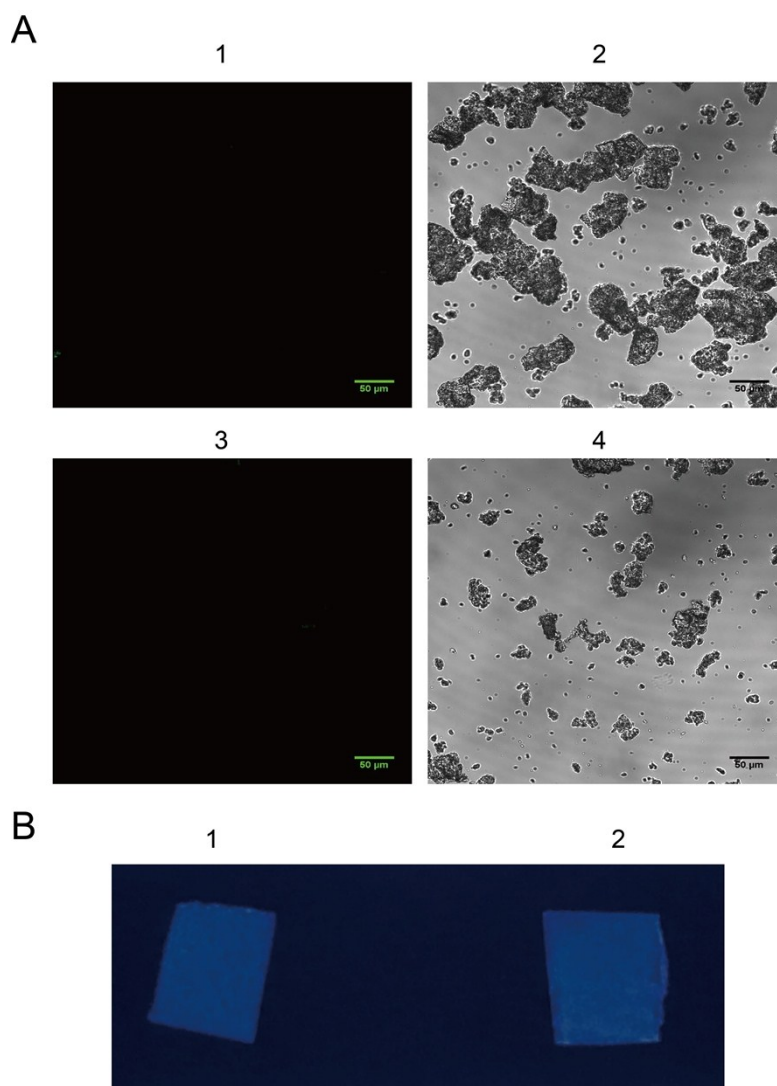


**Fig. S9** Negative controls of fluorescent capture images of *FfAA11*-treated chitins (**A**), and lobster shell (**B**). **A** Untreated chitin (A1) and *FfAA11*-treated but none PyBOP-activated FTSC conjugation (A3). The A2 and A4 are corresponding to bright-field images of A1 and A3, respectively. **B** UV light detection of FTSC on the surface of lobster shell: B1, Section of untreated lobster shell combined with COMU coupling reagent and FTSC; B2 *FfAA11*-treated but none COMU-activated FTSC conjugation.

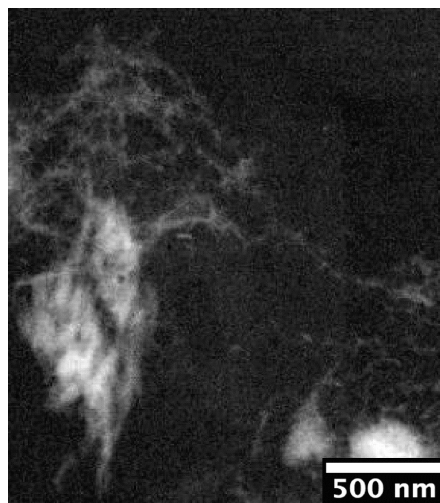


**Fig. S10** Non-activated *FfAA1* treated chitin and COMU activated coupling of gold nanoparticles.